ACCEPTED FOR PUBLICATION IN ASTROPHYSICAL JOURNAL LETTERS
Preprint typeset using LaTeX style emulateapj v. 6/22/04

THE FUNDAMENTAL PLANE FOR $z = 0.8-0.9$ CLUSTER GALAXIES

INGER JØRGENSEN[1], KRISTIN CHIBOUCAS[1], KATHLEEN FLINT[1,2], MARCEL BERGMANN[3], JORDI BARR[4], ROGER DAVIES[4]

Accepted for publication in Astrophysical Journal Letters

ABSTRACT

We present the Fundamental Plane (FP) for 38 early-type galaxies in the two rich galaxy clusters RXJ0152.7–1357 ($z = 0.83$) and RXJ1226.9+3332 ($z = 0.89$), reaching a limiting magnitude of $M_B = -19.8$ mag in the rest frame of the clusters. While the zero point offset of the FP for these high redshift clusters relative to our low redshift sample is consistent with passive evolution with a formation redshift of $z_{\rm form} \approx 3.2$, the FP for the high redshift clusters is not only shifted as expected for a mass-independent $z_{\rm form}$, but rotated relative to the low redshift sample. Expressed as a relation between the galaxy masses and the mass-to-light ratios the FP is significantly steeper for the high redshift clusters than found at low redshift. We interpret this as a mass dependency of the star formation history, as has been suggested by other recent studies. The low mass galaxies ($10^{10.3} M_\odot$) have experienced star formation as recently as $z \approx 1.35$ (1.5 Gyr prior to their look back time), while galaxies with masses larger than $10^{11.3} M_\odot$ had their last major star formation episode at $z > 4.5$.

Subject headings: galaxies: clusters: individual: RXJ0152.7–1357 – galaxies: clusters: individual: RXJ1226.9+3332 – galaxies: evolution – galaxies: stellar content.

1. INTRODUCTION

The Fundamental Plane (FP) for elliptical (E) and lenticular (S0) galaxies is a key scaling relation, which relates the effective radii, the mean surface brightnesses and the velocity dispersions in a relation linear in log-space (e.g., Dressler et al. 1987; Djorgovski & Davis 1987; Jørgensen et al. 1996, hereafter JFK1996). The FP can be interpreted as a relation between the galaxy masses and their mass-to-light (M/L) ratios. For low redshift cluster galaxies the FP has very low internal scatter, e.g. JFK1996. It is therefore a powerful tool for studying the evolution of the M/L ratio as a function of redshift (e.g., Jørgensen et al. 1999; Kelson et al. 2000; van de Ven et al. 2003; Gebhardt et al. 2003; Wuyts et al. 2004; Treu et al. 2005; Ziegler et al. 2005). These authors all find that the FP at z=0.2–1.0 is consistent with passive evolution of the stellar populations of the galaxies, generally with a formation redshift $z_{\rm form} > 2$. Most previous studies of the FP at z=0.2–1.0 cover fairly small samples of galaxies in each cluster and are limited to a narrow range in luminosities and therefore in masses, making it very difficult to detect possible differences in the FP slope. A few recent studies indicated a steepening of the FP slope for $z \sim 1$ galaxies (di Serego Alighieri et al. 2005; van der Wel et al. 2005; Holden et al. 2005). These studies and studies of the K-band luminosity function (Toft et al. 2004) and the red sequence (de Lucia et al. 2004) at $z \approx 0.8-1.2$ suggest a mass dependency of the formation epoch.

We present the FP for two galaxy clusters RXJ0152.7–1357 at $z = 0.83$ and RXJ1226.9+3332 at $z = 0.89$. Our samples reach apparent i'-band magnitudes of 22.5–22.8 mag, equivalent to an absolute magnitude of $M_B = -19.8$ mag in the rest frame of the clusters. No other published samples suitable for studies of the cluster galaxy FP at $z > 0.8$ go this deep. Our study of these two clusters is part of the Gemini/HST Galaxy Cluster Project, which is described in detail in Jørgensen et al. (2005). We adopt a ΛCDM cosmology with $H_0 = 70\,{\rm km\,s^{-1}\,Mpc^{-1}}$, $\Omega_M = 0.3$, and $\Omega_\Lambda = 0.7$.

[1] Gemini Observatory, 670 N. A'ohoku Pl., Hilo, HI 96720; ijorgensen@gemini.edu, kchibouc@gemini.edu

[2] Currently at State University of New York at Stony Brook, The Reinvention Center, Stony Brook, NY 11794; kathleen.flint@stonybrook.edu

[3] Gemini Observatory, La Serena, Chile; mbergmann@gemini.edu

[4] Department of Astrophysics, University of Oxford, Keble Road, Oxford OX1 3RH, UK; jmb@astro.ox.ac.uk, rld@astro.ox.ac.uk

2. OBSERVATIONAL DATA

Spectroscopy for RXJ0152.7–1357 and RXJ1226.9+3332 were obtained with the Gemini Multi-Object Spectrograph (GMOS-N, Hook et al. 2004) at Gemini North. The data for RXJ0152.7–1357 are published in Jørgensen et al. (2005). The reduction of the RXJ1226.9+3332 spectroscopy was done using similar techniques, with suitable changes to take into account the use of the nod-and-shuffle mode of GMOS-N (Jørgensen et al. in prep.). We use Hubble Space Telescope (HST) archive data of the two clusters obtained with the Advanced Camera for Surveys (ACS). In this paper we use effective radii, $r_{\rm e}$, and mean surface brightnesses, $\langle I \rangle_{\rm e}$, derived from either F775W or F814W observations, calibrated to rest-frame *B*-band, see Chiboucas et al. (in prep.) for details. The GALFIT program (Peng et al. 2002) was used to determine $r_{\rm e}$ and $\langle I \rangle_{\rm e}$. We fit the cluster members with Sérsic (1968) and $r^{1/4}$ profiles. The combination which enters the FP, $\log r_{\rm e} + \beta \log \langle I \rangle_{\rm e}$ (β =0.7-0.8), differs very little for the two choices of profiles. In the following we use the parameters from $r^{1/4}$-fits for consistency with our low redshift comparison data. None of the main conclusions of this paper would change had we chosen to use the Sérsic fits. Masses of the galaxies are derived as $Mass = 5\sigma^2 {\rm r_e\, G^{-1}}$.

Our Coma cluster sample serves as the low redshift reference sample (Jørgensen 1999). We have obtained new *B*-band photometry of this sample with the McDonald Observatory 0.8-meter telescope and the Primary Focus Camera (Claver 1995). The data were reduced in a standard fashion and effective parameters were derived as described in Jørgensen et al. (1995). Table 1 summarizes the sample sizes and some key cluster properties.

3. THE FUNDAMENTAL PLANE AT Z=0.8-0.9

We first establish the FP for the Coma cluster data. In order to limit the effect of differences in sample selection for

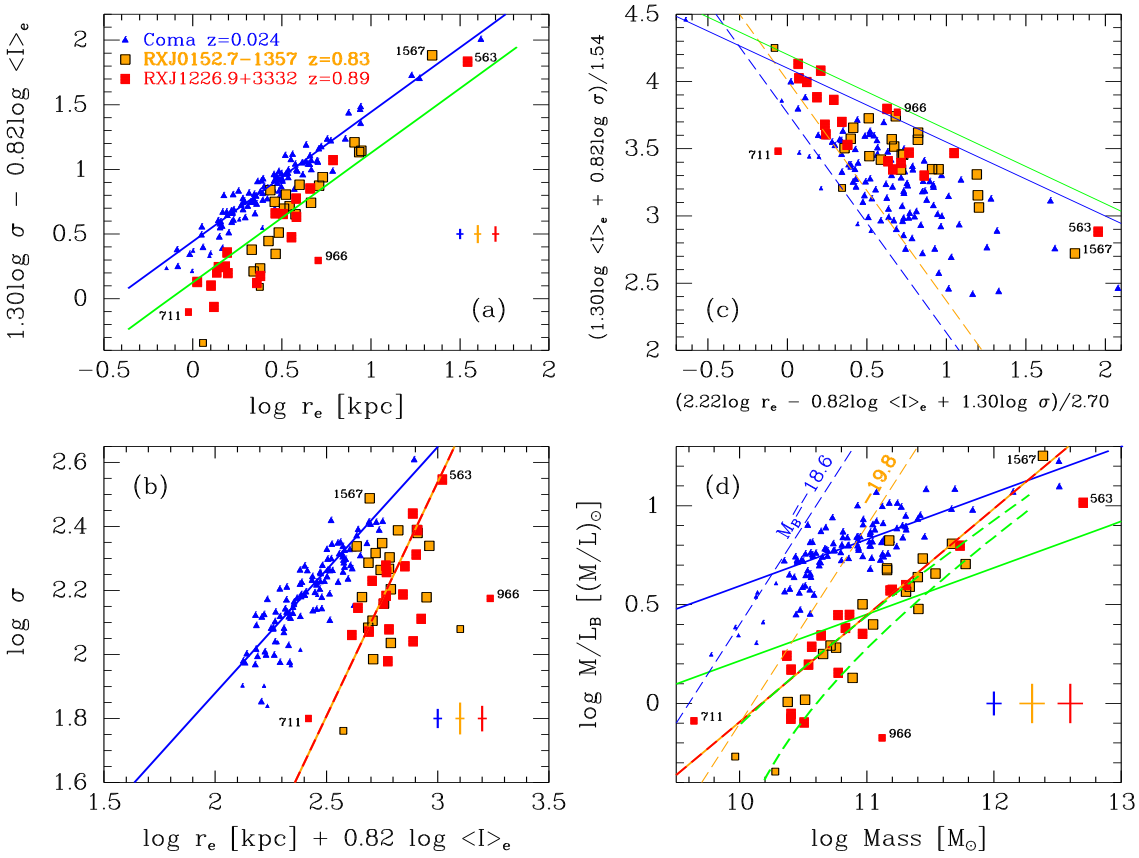

FIG. 1.— The FP for RXJ0152.7-0152 (orange), RXJ1226.9+3332 (red), and Coma (blue). Smaller symbols – galaxies with $Mass < 10^{10.3} M_{\odot}$, excluded from the analysis. RXJ1226.9+3332 id=711 and id=966 (with Sérsic index $n < 1.5$) are labeled and excluded from the analysis. (a) & (b): Edge-on view of the FP. (c): The FP face-on, for the Coma cluster coefficients. (d): The FP as Mass *vs.* M/L ratio. Solid blue line on (a), (b) & (d): Fit to the Coma cluster sample. Solid green line on (a) & (d): The Coma cluster fit offset to the median zero point of the high redshift sample. Orange-red line on (b) & (d): Fit to the high redshift sample. The fit shown on (b) is not the optimal FP for the high redshift sample, since it has the coefficient for $\log\langle I\rangle_e$ fixed at 0.82. Dashed lines on (c) and (d): Luminosity limits for the Coma cluster (blue), and both redshift clusters (orange). On (c) the solid blue and green lines mark the "exclusion zones" (Bender et al. 1992) for the Coma cluster and high redshift sample, respectively, assuming the slope and zero points as shown on (a). Dashed green lines on (d): Models from Thomas et al. (2005), see text for discussion. Internal uncertainties are shown as representative error bars. On (c) the internal uncertainties are the size of the points.

TABLE 1
GALAXY CLUSTERS AND SAMPLES

Cluster	Redshift	$\sigma_{\rm cluster}$[a]	$N_{\rm galaxies}$[b]	$N_{\rm analysis}$[c]	Ref.[d]
Coma=Abell1656	0.024	1010 km s^{-1}	116	105	(1)
RXJ0152.7–1357	0.835	1110 km s^{-1}	29	20	(2)
RXJ1226.7+3332	0.892	1270 km s^{-1}	25	18	(3)

[a]Cluster velocity dispersion
[b]Number of galaxies observed
[c]Number of galaxies included in the analysis, see text.
[d](1) Jørgensen 1999; (2) Jørgensen et al. 2005; (3) This paper

the Coma cluster sample and the high redshift sample, we exclude galaxies with $Mass < 10^{10.3} M_{\odot}$ as well as emission line galaxies. The sum of the absolute residuals perpendicular to the relation was minimized. We find

$$\log r_e = (1.30 \pm 0.08)\log\sigma - (0.82 \pm 0.03)\log\langle I\rangle_e - 0.443 \quad (1)$$

where r_e is the the effective radius in kpc, σ the velocity dispersion in km s^{-1}, and $\langle I\rangle_e$ is the surface brightness within r_e in $L_{\odot}$ pc^{-2}. The uncertainties on the coefficients are determined using a bootstrap method, see JFK1996 for details. The rms of the fit is 0.08 in $\log r_e$. The coefficients are in agreement with other determinations available in the literature (e.g., JFK1996; Colless et al. 2001; Blakeslee et al. 2002; Bernardi et al. 2003).

Figure 1 shows the Coma cluster FP face-on as well as two edge-on views of the relation, with the high redshift sample overplotted. The FP for the high redshift sample is not only offset from the Coma cluster FP, but appears "steeper". As there is no significant FP zero point difference between the two high redshift clusters we treat the high redshift galaxies as one sample. Deriving the FP for the high redshift sample using the same technique and sample criteria as for the Coma cluster, we find

$$\log r_e = (0.60 \pm 0.22)\log\sigma - (0.70 \pm 0.06)\log\langle I\rangle_e + 1.13 \quad (2)$$

with an rms of 0.09 in $\log r_e$. The difference in the coefficient for $\log\sigma$ between Eq. 1 and Eq. 2 is $\Delta\alpha = 0.70 \pm 0.23$, a 3σ detection of a difference in the FP slope. The internal scatter of the two relations is similar. Figure 1d shows the FP as a relation between the galaxy masses and the M/L ratios. The fit to the Coma sample, excluding the low mass galaxies, gives

$$\log M/L = (0.24 \pm 0.03)\log Mass - 1.75 \quad (3)$$

with an rms of 0.09 in $\log M/L$. Fitting the high redshift sample, using the same mass limit, gives

$$\log M/L = (0.54 \pm 0.08)\log Mass - 5.47 \qquad (4)$$

with an rms of 0.14 in $\log M/L$. The internal scatter in $\log M/L$ of the two relations are not significantly different. We find 0.07 and 0.08 for the Coma sample and the high redshift sample, respectively. Even with the same mass limit enforced on both samples one might argue that the fits are still affected by the difference in the luminosity limit. Therefore, we also fit a sub-sample of the Coma sample limited at $M_B = -19.8$ mag. The coefficient for $\log Mass$ is in this case 0.28 ± 0.06. Thus, the difference between the coefficients for the high redshift and the low redshift samples is at the 3σ level.

4. POSSIBLE SYSTEMATIC EFFECTS

To test how well we recover input r_e, $\langle I \rangle_e$ and $\log r_e + \beta \log \langle I \rangle_e$ (β =0.7-0.8), we simulate HST/ACS observations of galaxies with Sérsic profiles with $n = 0.8 - 4.6$ and effective parameters matching our Coma sample. For $n > 2$, the $r^{1/4}$-fits recover $\log r_e$ with an rms of 0.15. However, $\log r_e + \beta \log \langle I \rangle_e$ is recovered with an rms scatter of only ≈ 0.02 for β between 0.7 and 0.8. There are no systematic effects as a function of effective radii or luminosities, see Chiboucas et al. (in prep.) for details. Simulations of spectra matching the instrumental resolution, signal-to-noise ratios and spectral properties of our observational data showed that velocity dispersions below the instrumental resolution ($\log \sigma = 2.06$) may be subject to systematic errors as large as ± 0.15 in $\log \sigma$ (Jørgensen et al. 2005). Excluding from the analysis the four galaxies in the high redshift sample with $\log \sigma < 2.06$, we find a slope for the M/L ratio–mass relation of 0.47 ± 0.06, while the FP coefficients are not significantly different from those given in Eq. 2.

Finally, we address whether selection effects can be the cause of the differences in the relations for the two samples. We choose 1000 random sub-samples of 38 galaxies from the Coma sample, roughly matching the mass distribution of the high redshift sample. We confirm the match in mass distributions by using a Kolmogorov-Smirnov test. The probability that the sub-samples and the real high redshift sample are drawn from the same parent distribution is above 90% for more than 90% of the realizations. For the remainder the probability is above 70%. We then compare the fits to these sub-samples to the results from bootstrapping the high redshift sample. For the FP coefficients the sub-sample fits overlap the bootstrap fits in only 1.6% of the cases (Fig. 2a), while for the M/L ratio–mass relation the slope for the sub-samples overlap with the bootstrap fits in 3.7% of the cases (Fig. 2b). This shows that the FP and the M/L ratio–mass relation for the high redshift sample are different from the relations found for the Coma sample at the 96–98% confidence level.

Based on the simulations of the data and the selection effects, we conclude that the differences in relations we find between the Coma sample and the high redshift sample are unlikely to be due to systematic effects in the data or due to differences in selection effects.

5. THE STAR FORMATION HISTORY OF E/S0 CLUSTER GALAXIES

The median offset of $\log M/L$ for the high redshift sample relative to the Coma sample is –0.38. Using stellar population models from Maraston (2005), which show that

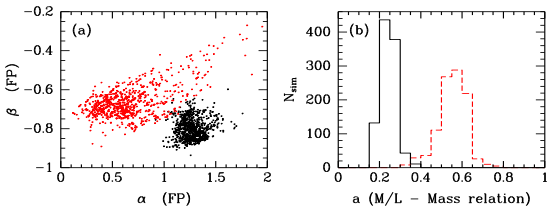

FIG. 2.— Distributions of FP coefficients and the slope, a, of the M/L ratio–mass relation for 1000 sub-samples of the Coma cluster sample (black) and for 1000 bootstrap samples of the high redshift sample (red, dashed). See text for discussion.

$\Delta \log M/L = 0.935 \Delta \log age$ (Jørgensen et al. 2005), this gives an epoch for the last major star formation episode of $z_{form} \approx 3.2$. However, the steeper M/L ratio–mass relation found for high redshift clusters compared to the Coma cluster may be due to a difference in the epoch of the last major star formation episode as a function of galaxy mass. The low mass galaxies have experienced the last major star formation episode much more recently than is the case for the high mass galaxies. The difference between the high and low redshift samples is $\Delta \log M/L = -0.30 \log Mass + 3.72$, equivalent to $\Delta \log age = -0.32 \log Mass + 4.0$. Thus, for the lowest mass galaxies ($10^{10.3} M_\odot$) the last epoch of star formation may have been as recent as $z_{form} \approx 1.35$. This is only $\approx$1.5 Gyr prior to when the light that we now observe was emitted from the galaxies in the high redshift sample. There appears to be just enough time for the galaxies to no longer have detectable emission lines due to the massive stars formed at that time. Very shortly after the end of the last major star formation episode these galaxies follow a tight FP. For galaxies with $Mass \approx 10^{10.8} M_\odot$ we find $z_{form} \approx 1.9$, while $z_{form} > 4.5$ for galaxies with $Mass > 10^{11.3} M_\odot$.

Thomas et al. (2005) used absorption line index data for nearby E/S0 galaxies to establish rough star formation histories of the galaxies as a function of their masses. They find that the most massive galaxies form the majority of their stars at high redshift, while lower mass galaxies continue forming stars at much later epochs. Thomas et al. convert velocity dispersions to galaxy masses using a model dependent relation that is inconsistent with our data. We therefore correct their masses to consistency with our data by using the empirical relation between our mass estimates and the measured velocity dispersions. The lower of the two dashed green lines on Figure 1d shows the result based on the star formation history in high density environments as established by Thomas et al. and the M/L modeling from Maraston (2005). Our data show slightly less evolution in the M/L ratios between $z \approx$0.8-0.9 and the present than predicted by Thomas et al. However, it is striking that the slope of the predicted relation is in agreement with our data. As an experiment we shifted the predictions from Thomas et al. to the best agreement with our data. The upper of the two dashed green lines show this for the formation look back times shifted 2.5 Gyr earlier for all masses such that the earliest formation look back time is 14 Gyr (roughly the age of the Universe in this cosmology). The absolute formation epochs from Thomas et al. may not be correct, since their analysis depends on stellar population models. However, their results on the relative timing of the star formation episodes as a function of galaxy mass closely match our results for this high redshift sample.

Thomas et al. predict that star formation is on-going for a longer period in low mass galaxies than in high mass galaxies.

Based on this, we estimate that the internal scatter in the M/L–mass relation, in $\log M/L$, should be ≈ 0.06 at $10^{10.3}\,M_{\odot}$ but only ≈ 0.01 at $10^{11.3}\,M_{\odot}$. We cannot confirm such a decrease of the internal scatter. However, it would most likely require a larger sample and/or significantly smaller measurement uncertainties to test this prediction.

Factors other than the mean ages of the stellar populations could be affecting the M/L ratios of the galaxies. For RXJ0152.7–1357 we found based on absorption line index data that a large fraction of the galaxies may have α-element abundance ratios, [α/Fe], about 0.2 dex higher than found in nearby clusters (Jørgensen et al. 2005). This could affect the M/L ratios in a systematic way. Maraston (private comm.) finds from modeling that stellar populations with [α/Fe] = 0.3, solar metallicities and ages of 2-7 Gyr may have M/L ratios in the blue that are about 20 per cent higher than those with [α/Fe] = 0.0. While it is still too early to use these models for detailed analysis of high redshift data, it indicates that for future detailed analysis of the FP we may have to include information about [α/Fe] of the galaxies.

6. CONCLUSIONS

We find that the FP for E/S0 galaxies in the clusters RXJ0152.7–1357 (z = 0.83) and RXJ1226.9+3332 (z = 0.89) is offset and rotated relative to the FP of our low redshift comparison sample of Coma cluster galaxies. Expressed as a relation between the M/L ratios and the masses of the galaxies, the high redshift galaxies follow a significantly steeper relation than found for the Coma cluster. We interpret this as due to a mass dependency of the epoch of the last major star formation episode. The lowest mass galaxies in the sample ($10^{10.3}\,M_{\odot}$) have experienced significant star formation as recent as $z_{\rm form} \approx 1.35$, while high mass galaxies ($Mass > 10^{11.3}\,M_{\odot}$) have $z_{\rm form} > 4.5$. This is in general agreement with the predictions for the star formation histories of E/S0 galaxies from Thomas et al. (2005) based on their analysis of line index data for nearby galaxies. The scatter of FP for these two $z = 0.8-0.9$ clusters is as low as found for the Coma cluster, and we find no significant difference in the scatter for low and high mass galaxies. This indicates that at a given galaxy mass the star formation history for the E/S0 galaxies is quite similar. In a future paper we will discuss these results in connection with our absorption line index data for the galaxies in both high redshift clusters.

Based on observations obtained at the Gemini Observatory (GN-2002B-Q-29, GN-2004A-Q-45), which is operated by AURA, Inc., under a cooperative agreement with NSF on behalf of the Gemini partnership: NSF (US), PPARC (UK), NRC (Canada), CONICYT (Chile), ARC (Australia), CNPq (Brazil) and CONICET (Argentina). Based on observations made with the NASA/ESA Hubble Space Telescope. IJ, KC, and KF acknowledge support from grant HST-GO-09770.01 from STScI. STScI is operated by AURA, Inc. under NASA contract NAS 5-26555.

REFERENCES

Bender, R., Burstein, D., & Faber, S. M. 1992, ApJ, 399, 462
Bernardi, M., et al. 2003, AJ, 125, 1866
Blakeslee, J. P., Lucey, J. R., Tonry, J. L., Hudson, M. J., Narayanan, V. K., & Barris, B. J. 2002, MNRAS, 330, 443
Claver, C. F. 1995, Ph. D. thesis, Univ. Texas
Colless, M., Saglia, R. P., Burstein D., Davies, R. L., McMahan Jr., R. K., & Wegner, G. 2001, MNRAS, 321, 277
de Lucia, G., et al. 2004, ApJ, 610, L77
di Serego Alighieri, S., et al. 2005, A&A, 442, 125
Djorgovski, S., & Davis, M. 1987, ApJ, 313, 59
Dressler, A., Lynden-Bell, D., Burstein, D., Davies, R. L., Faber, S. M., Terlevich, R., Wegner G. 1987, ApJ, 313, 42
Gebhardt, K., et al. 2003, ApJ, 597, 239
Holden, B. P., et al. 2005, ApJ, 620, L83
Hook, I. M., Jørgensen, I., Allington-Smith, J. R., Davies, R. L., Metcalfe, N., Murowinski, R. G., & Crampton, D. 2004, PASP, 116, 425
Jørgensen, I. 1999, MNRAS, 306, 607
Jørgensen I., Franx M., & Kjærgaard, P. 1995, MNRAS, 273, 1097
Jørgensen, I., Franx, M., & Kjærgaard, P. 1996, MNRAS, 280, 167 (JFK1996)
Jørgensen, I., Franx, M., Hjorth, J., & van Dokkum, P. G. 1999, MNRAS, 308, 833
Jørgensen, I., Bergmann, M., Davies, R., Jordi, B., Takamiya, M., & Crampton, D. 2005, AJ, 129, 1249
Kelson, D. D., Illingworth, G. D., van Dokkum, P. G., & Franx, M. 2000, ApJ, 531, 184
Maraston, C. 2005, MNRAS, 362, 799
Peng, C. Y., Ho, L. C., Impey, C. D., & Rix, H.-W. 2002, AJ, 124, 266
Sérsic, J. L. 1968, Atlas de Galaxias Australes (Córdoba: Obs. Astron. Univ. Nac. Córdoba)
Thomas, D., Maraston, C., Bender, R., & de Oliveira, C. M. 2005, ApJ, 621, 673
Toft, S., Mainieri, V., Rosati, P., Lidman, C., Demarco, R., Nonino, M., & Stanford, S. A. 2004, A&A, 422, 29
Treu, T., et al. 2005, ApJ, 633, 174
van der Wel, A., Franx, M., van Dokkum, P. G., Rix, H.-W., Illingworth, G. D., & Rosati, P. 2005, ApJ, 631, 145
van de Ven, G., van Dokkum, P. G., & Franx, M. 2003, MNRAS, 344, 924
Wuyts, S., van Dokkum, P. G., Kelson, D. D., Franx, M., & Illingworth, G. D. 2004, ApJ, 605, 677
Ziegler, B. L., Thomas, D., Böhm, A., Bender, B., Fritz, A., & Maraston, C. 2005, A&A, 433, 519